

# Ocellar spatial vision in *Myrmecia* ants

Bhavana Penmetcha<sup>\*1</sup>, Yuri Ogawa<sup>\*1,2</sup>, Laura A. Ryan<sup>1</sup>, Nathan S. Hart<sup>1</sup>, Ajay Narendra<sup>1,3</sup>

<sup>1</sup> Department of Biological Sciences, Macquarie University, Sydney, NSW 2109, Australia.

<sup>2</sup> Centre for Neuroscience, Flinders University, GPO Box 2100, Adelaide, SA 5001, Australia.

<sup>3</sup> Corresponding author: [ajay.narendra@mq.edu.au](mailto:ajay.narendra@mq.edu.au)

\*Equal first authors

## Summary statement

Electrophysiological techniques reveal that spatial visual properties of simple eyes improves with input from compound eyes in bull ants and honeybees.

## Abstract

In addition to the compound eyes, insects possess simple eyes known as ocelli. Input from the ocelli modulates optomotor responses, flight-time initiation, and phototactic responses—behaviours that are mediated predominantly by the compound eyes. In this study, using pattern electroretinography (pERG), we investigated the contribution of the compound eyes to ocellar spatial vision in the diurnal Australian bull ant *Myrmecia tarsata* by measuring the contrast sensitivity and spatial resolving power of the ocellar second-order neurons under various occlusion conditions. Furthermore, in four species of *Myrmecia* ants active at different times of the day, and in European honeybee *Apis mellifera*, we characterized the ocellar visual properties when both visual systems were available. Among the ants, we found that the time of activity had no significant effect on ocellar spatial vision. Comparing day-active ants and the honeybee we did not find any significant effect of locomotion on ocellar spatial vision. In *M. tarsata*, when the compound eyes were occluded, the amplitude of the pERG signal from the ocelli reduced by three times compared to conditions when the compound eyes were available. The signals from the compound eyes maintained the maximum contrast sensitivity of the ocelli as 13 (7.7%), and the spatial resolving power as

0.29 cpd. We conclude that ocellar spatial vision improves significantly with input from the compound eyes, with a noticeably larger improvement in contrast sensitivity than in spatial resolving power.

**Keywords:** pattern electroretinography; flying; walking; bull ants; honeybees; contrast sensitivity; spatial resolving power

## Introduction

Insects use vision to detect relevant information from their environment to orient themselves, find conspecifics, forage, navigate, hunt and mate (Cronin et al., 2014). While the compound eyes have been studied extensively (e.g., Greiner, 2006; Land, 1989; Narendra et al., 2017; Warrant, 2008), many insects also possess a single-lens type eye known as an ocellus which has been relatively understudied (e.g., Mizunami, 1995; Ribi and Zeil, 2018; Warrant et al., 2006). Typically, three simple eyes are placed in a triangular formation on the dorsal surface of the head. Each ocellus consists of a lens, an iris, a corneaceous cell layer, and a retina differentiated into dorsal and ventral retinæ (Narendra and Ribi, 2017; Ribi and Zeil, 2018; Ribi et al., 2011). Almost all flying insects possess ocelli. Their functions have been best studied in dragonflies and locusts where the ocelli play a crucial role in horizon detection (Berry et al., 2007a; Stange et al., 2002) and attitude control during flight (Mizunami, 1995; Stange, 1981; Taylor, 1981; Wilson, 1978). In addition, input from the ocelli aids visually guided behaviours such as flight time initiation (Eaton et al., 1983; Lindauer and Schricker, 1963; Schricker, 1965; Wellington, 1974), optomotor responses (Honkanen et al., 2018) and phototactic responses (Barry and Jander, 1968; Cornwell, 1955). Ocelli are typically absent in walking insects; exceptions include the workers of desert ants of the genera *Cataglyphis* and *Melophorus* (Penmetcha et al., 2019; Schwarz et al., 2011a), and bull ants or jack jumpers of the genus *Myrmecia* (Narendra and Ribi, 2017; Narendra et al., 2011). Behavioural evidence shows that the ocelli of the desert ants derive compass information from celestial cues (Schwarz et al., 2011b; Schwarz et al., 2011c), especially the pattern of polarized skylight (Fent and Wehner, 1985; Mote and Wehner, 1980).

Neuroanatomical studies have confirmed interactions between the ocelli and the compound eye, specifically between the large second-order neurons (L-neurons) that receive input from a large number of ocellar photoreceptors and the optic lobe where signals from the compound eyes are processed. For example, in honeybees and flies, efferent fibres run from

the lobula plate into the ocellar tract (Strausfeld 1976, see also Hagberg and Nässel 1986). In the European field cricket *Gryllus campestris*, fibres run from the medulla to the ocellar tract forming knob-like blebs (Honegger and Schürmann, 1975). In the Australian field cricket *Teleogryllus commodus* and house cricket *Acheta domesticus* neurons extend from the ocellar photoreceptors to the lobular layers of the compound eyes and additionally in the laminar layers of *T. commodus* (Rence et al., 1988). Physiological studies in *T. commodus* showed that the amplitude of the electroretinograms (ERGs) measured from the compound eyes was reduced by 20% following ocellar occlusion (Rence et al., 1988). However, it is unknown whether the visual information received by the compound eyes has an effect on the visual capabilities of the ocelli.

The capabilities of a visual system are determined by the extent to which it can discriminate between fine details of objects in a scene (spatial resolving power) and adjacent stimuli based on differences in relative luminosity (contrast sensitivity) (Land, 1997). The image quality of ocellar lenses have been estimated histologically, using the hanging drop technique (originally described by Homann, 1924) and modifications of this technique. Histological evidence suggests that in some insects the ocellar lenses likely produce under-focused images because the focal plane is located behind the retina in migratory locusts *Locusta migratoria* (Berry et al., 2007b; Wilson, 1978), sweat bees *Megalopta genalis* (Warrant et al., 2006), blowflies *Calliphora erythrocephala* (Cornwell, 1955; Schuppe and Hengstenberg, 1993), orchid bees *Euglossa imperialis* (Taylor et al., 2016) and Indian carpenter bees *Xylocopa leucothorax*, *X. tenuiscapa*, and *X. tranquebarica* (Somanathan et al., 2009). In some insects the ocelli appear to be capable of resolving images with the plane of best focus located close to the retina as seen in European honeybees *Apis mellifera* (Ribi et al. 2011, but see Hung and Ibbotson 2014), paper wasps *Apoica pallens* and *Polistes occidentalis* (Warrant et al., 2006), and dragonflies *Hemicordulia tau* and *Aeshna mixta* (Berry et al., 2007c; Berry et al., 2007a; Stange et al., 2002). Additionally, the spatial resolution of the honeybee ocelli was estimated by quantifying the contrast in the image produced by the lens (Hung and Ibbotson, 2014) and that of the dragonfly ocelli by measuring the acceptance angles of the ocellar photoreceptors (Berry et al., 2007c). In honeybees, when provided with vertical and horizontal gratings, it was found that contrast information for high spatial frequency was transferred through the ocellar lenses better than low spatial frequency (Hung and Ibbotson, 2014). In dragonflies, the acceptance angles were obtained by ray tracing through anatomical models of the median ocellar lens and retina. The

acceptance angle in elevation ( $5.2^\circ$ ) was half that in azimuth ( $10.3^\circ$ ) suggesting higher resolution in the vertical plane (Berry et al., 2007c).

The hanging drop technique and other histological methods do not consider the physiological properties of the photoreceptors or the ocellar second-order neurons, which are essential for determining the visual capabilities of the eye. Hence, intracellular electrophysiology has been used to infer the spatial resolution of the ocelli. In dragonflies, the spatial resolution of the ocelli was extrapolated by measuring the angular sensitivities of the median ocelli photoreceptors (van Kleef et al., 2005) and ocellar second-order neurons (Berry et al., 2006; Berry et al., 2007a) in response to green and ultra-violet (UV) LED arrays. Similar experiments were done on the second-order neurons in the lateral ocelli of locusts (Wilson, 1978) in response to a Xenon arc lamp. In dragonfly median ocelli, the acceptance angles of the photoreceptors were  $15^\circ$  in elevation and  $28^\circ$  in the azimuth, in the vertical and horizontal plane respectively indicating relatively enhanced spatial resolution in the vertical plane (van Kleef et al., 2005). These values were a factor of 2 or more larger than when obtained from the ray tracing method mentioned previously (Berry et al., 2007c). Additionally, although the acceptance angles were slightly higher (elevation =  $20^\circ$ , azimuth =  $40^\circ$ ) when measured from the ocellar second-order neurons, the hypothesis of enhanced spatial resolution in the vertical plane remains unchanged; providing evidence that spatial resolution is conserved after convergence of photoreceptors onto second-order neurons (Berry et al., 2006). In locusts, angular sensitivities were measured only in the horizontal plane and it was found that the field widths measured at 50% maximum sensitivity showed considerable variation. However, the total extent of the field for all the cells showed less variation and was at least  $130^\circ$  indicating that the spatial resolution was low in these neurons (Wilson, 1978). Therefore, while the spatial resolution of the ocelli has been estimated using various techniques, the contrast sensitivity of the ocelli has neither been estimated nor measured physiologically (but see Simmons, 1993 for intracellular responses of L-neurons to sinusoidally modulated light of varying contrasts in locusts).

Pattern electroretinography (pERG) has been used to measure simultaneously the spatial resolving power and contrast sensitivity of the compound eyes in ants (Ogawa et al., 2019; Palavalli-Nettimi et al., 2019) and honeybees (Ryan et al., 2020). The pERG consists of non-linear ERG components that are generated by second-order visual neurons, at least in vertebrates (Porciatti, 2007), in response to contrast-reversing sinusoidal gratings that are contrast-modulated patterned visual stimuli at constant mean luminance. In insects, when measured in the presence of ON and OFF light stimuli, ERGs from the compound eyes show

the presence of ON transients (Coombe, 1986; Ryan et al., 2020) and OFF transients (Coombe, 1986; Palavalli-Nettimi et al., 2019; Ryan et al., 2020) arising from the second-order neurons in the lamina. Conventional electroretinograms (ERGs) recorded from the ocelli of cockroaches and dragonflies show the presence of Component 3, a hyperpolarizing post-synaptic potential (particularly prominent in dragonflies (Ruck, 1961a)) and a sustained after-potential (shown only in dragonflies (Ruck, 1961b)) arising from the dendrites of the ocellar nerve fibres (ocellar second-order neurons). This finding was predominantly based on the relative magnitudes of the ERG components recorded from the two ends of the ocellus: the photoreceptor layer and the ocellar nerve fibres (Ruck, 1961a; Ruck, 1961b). Alternatively, Component 3 can also be described as a small negative-going wave when measured at the cornea. Hence, the pERG technique is ideal as it allows us to simultaneously determine the spatial resolving power and contrast sensitivity.

Ants of the genus *Myrmecia* are unusual, as closely related congeneric species are active at different times of the day (Greiner et al., 2007; Narendra et al., 2011). Each species has evolved distinct adaptations in their compound eyes (Greiner et al., 2007; Narendra et al., 2011; Narendra et al., 2017; Ogawa et al., 2019) and ocelli (Narendra and Ribi, 2017; Narendra et al., 2011) to suit the specific temporal niches they occupy. The ocelli of night-active *Myrmecia* ants tend to have larger lenses and wider rhabdoms to improve optical sensitivity (Narendra and Ribi, 2017). Among worker ants, *Myrmecia* have relatively large ocelli which makes this group ideal to investigate ocellar physiology in day- and night-active ants.

In this study, we determined the contribution of the compound eyes to ocellar spatial vision using the pERG technique. We measured contrast sensitivity and spatial resolving power of the ocellar second-order neurons in the diurnal-crepuscular *Myrmecia tarsata* under different visual system occlusion conditions. Next, we measured the ocellar visual properties in four *Myrmecia* species to explore the effect of activity time on ocellar spatial vision. Lastly, to identify the effect of locomotory style on spatial vision we compared the ocellar visual properties of diurnal walking *Myrmecia* ants to the diurnal flying honeybee, *Apis mellifera*.

## Methods

### *Study Species*

We studied the physiology of the median ocelli in workers of four *Myrmecia* ant species: diurnal-crepuscular *Myrmecia gulosa* Fabricius (Sheehan et al., 2019) and *Myrmecia tarsata* Smith (Greiner et al., 2007); and the strictly nocturnal *Myrmecia midas* Clark (Freas et al., 2017) and *Myrmecia pyriformis* Smith (Greiner et al., 2007; Narendra et al., 2010). To identify whether ocellar spatial vision is influenced by locomotory differences, we compared the spatial properties of the day-active worker ants that have a pedestrian lifestyle with that of the workers of the day-active European honeybee *Apis mellifera* Linnaeus that predominantly fly. The animals were captured from multiple nests at the following locations: *M. midas*, *M. tarsata* and *A. mellifera* from the Macquarie University campus, North Ryde, NSW (33°46'10.24"S, 151°06'39.55"E); *M. gulosa* from Western Sydney University Hawkesbury campus, Richmond, NSW (33°37'46.35"S, 150°46'04.47"E); *M. pyriformis* from the Australian National University campus, Acton, ACT (35°16'50"S, 149°06'43"E). Working with insects requires no ethics approval in Australia.

### *Animal preparation*

To perform electrophysiological recordings, the ants were anesthetized by cooling them in an icebox for 5-10 mins before removing their antennae, legs and gaster. Each animal was then fixed horizontally onto a plastic stage with its dorsal side facing upwards using beeswax. The orientation of the median ocelli varies slightly between species (Narendra and Ribi, 2017). For instance, in *M. midas* and *M. pyriformis* the median ocelli are upward-facing, whereas in *M. tarsata* and *M. gulosa* the median ocelli are forward-facing. In addition, median ocelli are overall more upward- and forward-facing than the lateral ocelli in ants (Narendra et al., 2011; Penmetcha et al., 2019). Hence, in our preparations we oriented the head to ensure that only the median ocellus faced the stimulus. To place an active electrode on the median ocellar retina, a sharp blade was used to thin the cuticle immediately posterior to the median ocellar lens until the retina was visible. Vaseline (Unilever, USA) was placed on the thinned cuticle to prevent dehydration and a layer of conductive gel (Livingstone International Pty Ltd., New South Wales, Australia) was added. The honeybees were prepared similar to the ants after anesthetizing, following which their wings and legs were removed. The hair around the median ocellus was removed using sharp forceps for easier access to the retina and placement of electrode. In the honeybees, manual thinning of

the cuticle was not required as it is sufficiently thin that the electrode can receive signals from the retina.

The animals were mounted within a Faraday cage wherein electrophysiological recordings were carried out on the median ocellar retinae. An active electrode of platinum wire of 0.25mm diameter with a sharp tip was placed at the point where the cuticle was thinned, posterior to the median ocellar lens in the ants. In the honeybees the active electrode was placed on the cuticle, posterior to the median ocellar lens to access the retina underneath. The active electrode was immersed in the conductive gel in both cases. A silver/silver-chloride wire of 0.1mm diameter was inserted into the mesosoma of the ants and the thorax of the honeybees which served as an indifferent electrode.

To reduce any effects of the circadian rhythms on eye physiology, the experiments were conducted at the activity time of each species, i.e., from 1-6 hours post-sunset for nocturnal species and 2-8 hours post-sunrise for the diurnal species.

### ***Electroretinogram***

Using conventional electroretinography we measured the ON-OFF responses from the median ocelli in *M. tarsata* (n=5) to confirm the presence of extracellular potentials produced by the ocellar second-order neurons in electroretinograms (ERGs).

A white LED light source (5mm in diameter with irradiance of  $5.81 \times 10^{-5} \text{ W cm}^{-2}$ , C503C-WAS-CBADA151, Cree Inc., Durham, NC, USA) was used as a stimulus and placed 15 cm from the ocelli. The ants were dark-adapted for five minutes prior to stimulation. Ten consecutive trials were carried out, each trial lasting for ten seconds with the ON-OFF LED light stimulus presented after an initial delay of 0.5 seconds and for a total ON duration of five seconds using a custom-written script in MATLAB (R2015b, Mathworks, Natick, MA, US). The signals were filtered between 0.1 Hz – 100 Hz and amplified at  $\times 100$  gain (AC) using a differential amplifier (DAM50, World Precision Instruments Inc., FL, USA).

Certain ocellar second-order neurons (L-neurons) are known to form synapses with the descending interneurons which receive input from the compound eyes ((Strausfeld, 1976; *Apis mellifera* (Guy et al., 1979); *Schistocera gregaria*, *Schistocera americana* (Rowell and Pearson, 1983); *Calliphora erythrocephala* (Strausfeld and Bassemir, 1985)). Hence, we measured the ERGs from the median ocelli retina of *M. tarsata* for individuals with both visual systems-intact ( $E^+O^+$ ; n=5), and again with their compound eyes-occluded ( $E^-O^+$ , n=5).

These two experiments were conducted on the same individual consecutively and in random order without disturbing the placement of the electrode. Occlusion was done by applying a layer of opaque black nail enamel (B Beauty, NSW, Australia), which could be peeled off completely without damaging the eye or leaving any visible residue.

### ***Pattern electroretinogram (pERG)***

We used pattern electroretinography to measure the spatial resolving power and the contrast sensitivity of the ocelli of *Myrmecia* ants and *Apis mellifera* (n=4 for *M. gulosa*, n=5 for all other species).

The pERG visual stimuli were projected by a digital light-processing (DLP) projector (W1210ST, BenQ corporation, Taipei, Taiwan) onto a white screen (W51 x H81cm) at a distance of 30 cm from the animal. The stimuli were vertical contrast-reversing sinusoidal gratings of different spatial frequencies (cpd: cycles per degree) and Michelson's contrasts. They were generated using Psychtoolbox 3 (Pelli, 1997) and MATLAB (R2015b, Mathworks, Natick, MA, US) and controlled via a custom Visual Basic Software written in Visual Studio (2013, Microsoft Corporation, Redmond, WA, US). The mean irradiance of the grating stimulus was  $1.75 \times 10^{-4} \text{ W/cm}^2$  which was measured using a calibrated radiometer (ILT1700, International Light Technologies, Peabody, MA, US). A temporal frequency (frequency at which different spatial frequencies were presented) of 4 Hz was used for all the stimuli.

Prior to the first recording the animal was adapted to a uniform grey stimulus with the same mean irradiance as the grating stimuli for 20 minutes. To measure the contrast sensitivity function of the ocelli, nine spatial frequencies (0.05, 0.1, 0.15, 0.2, 0.26, 0.31, 0.36, 0.41, 0.52 cpd) and five contrasts (95%, 50%, 25%, 12.5%, 6%) for each spatial frequency were presented. The spatial frequencies were first presented in decreasing order of frequencies (0.52, 0.36, 0.26, 0.15, 0.05 cpd), skipping one frequency in between. In order to evaluate any degradation in response over time the interleaved frequencies were then presented in ascending order (0.1, 0.2, 0.31, 0.41 cpd). At each spatial frequency, all five contrasts were tested in decreasing order. Each combination of the stimuli was recorded for fifteen repeats, five seconds each and averaged in the time domain. The averaged responses were then analysed using a Fast Fourier Transform (FFT) in the frequency domain. As a control, the non-visual electrical signal (background noise) was recorded at two spatial frequencies (0.05 and 0.1 cpd) at 95% contrast with a black board to shield the animal from

the visual stimuli before and after running the experimental series. The maximum signal out of four control runs was used as the noise threshold.

### ***Contribution of the two visual systems to the pERG response amplitude in *M. tarsata****

To identify the origin of the neural responses recorded in the pERG, we compared the pERG response amplitudes in *M. tarsata* measured at each of the nine spatial frequencies (at 95% contrast) under different conditions: (a) both visual systems-intact ( $E^+O^+$ ) (n=5), (b) ocelli-occluded ( $E^+O^-$ ) (n=3), (c) compound eyes-occluded ( $E^-O^+$ ) (n=4) and (d) visual systems-intact with incisions in the lamina ( $E^+O^+L^-$ ) (n=3). In condition d, we made a rectangular window on the dorso-frontal region of both compound eyes using a sharp blade. We then accessed the lamina and made incisions on the basement membrane on both sides of the retinæ using a sharp blade. The windows were subsequently covered with Vaseline to prevent dehydration and the recordings performed. Following the electrophysiological recordings, we removed the cuticle and the brain was observed under a stereo microscope (Leica M205FA at 140x; Leica Microsystems Pty Ltd, Sydney, Australia). The incision was confirmed by two investigators. Occlusions were done as mentioned above. Condition d was performed to explore the effectiveness of our method of occlusion to block the compound eyes' input to the ocellar second-order neurons.

### ***Data analysis***

#### ***Spatial resolving power and contrast threshold***

To assess whether the pERG response signal at the second harmonic frequency (8Hz) of the FFT response spectrum differed significantly from 10 neighbouring frequencies, five on either side, for each spatial frequency and contrast combination, an F-test was used. The pERG amplitude was labelled as a significant data point if it differed significantly from the 10 neighbouring frequencies and labelled as a non-significant data point if not different. Only significant points were used to measure contrast sensitivity and spatial resolving power. The point at which the interpolation of the pERG response amplitudes above and below the noise threshold, intersects with the noise threshold are taken as the contrast threshold and the spatial resolving power. The contrast threshold at each spatial frequency of grating was used to calculate the contrast sensitivity at that particular spatial frequency, this being the reciprocal of the contrast threshold (See Ogawa et al., 2019 for more details).

### Statistical Analysis

We used a linear mixed-effects model in RStudio (R Core Team, 2018) to test whether the spatial frequency of the stimulus and the treatment conditions ( $E^+O^+$ ,  $E^+O^-$ ,  $E^-O^+$ ,  $E^+O^+L^-$ ) had an effect on the pERG response amplitudes (significant and non-significant points) in *M. tarsata*. The spatial frequency of the stimulus and the treatment conditions were the fixed effects, and animal identity was a random effect. The significances of the fixed effect terms were examined using Type III ANOVA. Both pERG response amplitudes and the spatial frequency data were log-transformed before the analysis and the final residuals were plotted and met the model assumptions.

To assess the effect of treatment condition ( $E^+O^+$ ,  $E^+O^-$ ) and stimulus spatial frequency on the contrast sensitivity function in *M. tarsata*, we used a linear mixed-effects model in R. The condition and the spatial frequency were the fixed effects and animal identity was a random effect. Using a linear model, we tested whether the spatial resolving power and the maximum contrast sensitivity differed between the two conditions. The contrast sensitivity and spatial frequency data were log-transformed before the data analysis. Final residuals of the data were plotted and met the model assumptions.

Lastly, we used a linear model to test whether the maximum contrast sensitivities differed between the four *Myrmecia* species, and the spatial resolving powers differed among the four *Myrmecia* species and *Apis mellifera*. A linear mixed-effects model was used to assess the effect of species, their time of activity and spatial frequency of stimulus on the contrast sensitivity function of the four *Myrmecia* species using a maximum likelihood (ML) estimation method. The same was done among diurnal *Myrmecia* ants and *Apis mellifera* to assess the effect of the species and their mode of locomotion on the contrast sensitivity functions. Time of activity in ants, spatial frequency, and locomotion were used as fixed effects, and animal identity nested within species was used as a random effect. The significances of the fixed effect terms were examined using the t-test with Satterthwaite approximation for degree of freedom (lmerTest package). The model also reflected the variability in the dependent variable (contrast sensitivity function) due to the random effects. The contrast sensitivity and spatial frequency data were log-transformed before the data analysis and the final residuals of the data were plotted and met the model assumptions. All linear-mixed effect models were carried out in the *lme4* package (Bates et al 2015) of R (<https://cran.r-project.org/web/packages/lme4/index.html>) using *lmer*.

## Results

### Electroretinogram

We first recorded ERGs to ON-OFF LED stimuli from the median ocelli of *M. tarsata* under two treatment conditions:  $E^+O^+$  (pink line in Fig. 1) and  $E^-O^+$  (black line in Fig. 1) to confirm the presence of the extracellular potentials originating from the ocellar second-order neurons. In  $E^+O^+$  condition (pink line in Fig. 1B, C) we identified at the stimulus onset, Component 3, a hyperpolarizing post-synaptic potential (arrow in Fig. 1B) and the sustained after-potential of Component 3 was also identified at the stimulus offset (arrow in Fig. 1C). However, in  $E^-O^+$  treatment condition (black line in Fig. 1B, C) Component 3 was identified at the stimulus offset (arrow in Fig. 1C) but was absent at the stimulus onset (dashed arrow Fig. 1B).

### Contribution of the two visual systems to the pERG response amplitude in *M. tarsata*

We measured the pERG response amplitudes from the ocellar second-order neurons in *M. tarsata* for each spatial frequency at 95% contrast. To confirm whether the ocellar second-order neurons receive inputs from the compound eyes in addition to the ocellar photoreceptors, we compared the response amplitudes in  $E^+O^+$ ,  $E^-O^+$ ,  $E^+O^-$  and  $E^+O^+L^-$  individuals (Fig. 2A, B, C, D). The spatial frequency of the visual stimuli and the treatment conditions had a significant effect on the response amplitudes (Type III ANOVA of linear-mixed effect model, parameter=treatment condition,  $df=3$ ,  $F=3.31$ ,  $P=0.03$ ; parameter=spatial frequencies,  $df=1$ ,  $F=141.23$ ,  $P<2.2e-16$ ; parameter=treatment condition:spatial frequency,  $df=3$ ,  $F=19.51$ ,  $P=4.06e-10$ ). For  $E^+O^+$ ,  $E^-O^+$  and  $E^+O^-$  treated individuals, the response amplitudes decreased with increasing spatial frequencies (slope for  $E^+O^+=-1.06$ ,  $E^-O^+=-0.62$ ,  $E^+O^-=-1.32$ ,  $E^+O^+L^-=0.02$ ) (Fig. 2A, B, C). The response amplitudes for  $E^+O^+$  individuals were significantly different from the  $E^+O^+L^-$  (Linear-mixed effect model,  $t=6.24$ ,  $P=9.5e-09$ ) and  $E^-O^+$  ( $t=2.7$ ,  $P=0.008$ ) treated individuals. Similarly, response amplitudes for  $E^+O^-$  treated individuals were significantly different from  $E^+O^+L^-$  ( $t=7.1$ ,  $P=2.34e-10$ ) and  $E^-O^+$  ( $t=3.85$ ,  $P=0.0002$ ) treated individuals. Additionally, the response amplitudes were significantly different between  $E^+O^+L^-$  and  $E^-O^+$  ( $t=-3.37$ ,  $P=0.001$ ) treated individuals but not significantly different between  $E^+O^+$  and  $E^+O^-$  ( $t=-1.59$ ,  $P=0.12$ ) treated individuals. However, at the lowest spatial frequency (0.05cpd), a linear model of the pERG response amplitudes for  $E^+O^+$  and  $E^+O^-$  treated individuals as a function of treatment conditions showed that the pERG response amplitudes were close to being significantly different between the two treatment conditions ( $F_{1,7}=5.51$ ,  $P=0.05$ ). The mean pERG response

amplitudes at the lowest spatial frequency (0.05cpd) for  $E^+O^+$  was  $0.009 \pm 0.0015$  (mean  $\pm$  S.E.) mV (Fig. 2A), for  $E^-O^+$  was  $0.003 \pm 0.0002$  mV (Fig. 2B), for  $E^+O^-$  was  $0.016 \pm 0.0018$  mV (Fig. 2C) and for  $E^+O^+L^-$  was  $0.001 \pm 0.0005$  mV (Fig. 2D).

### **Spatial properties in visual systems-intact and ocelli-occluded individuals of *M. tarsata***

We measured contrast sensitivities and the spatial resolving powers in  $E^+O^+$  and  $E^+O^-$  treated individuals (Fig. 3). At each spatial frequency of the visual stimuli, the amplitude of the pERG response decreased with decreasing contrast. The contrast sensitivity decreased as the spatial frequency increased under both the treatment conditions (Fig. 3A, Table 2). The maximum contrast sensitivities attained at the lowest spatial frequency (0.05cpd) was  $12.9 \pm 1.2$  (mean  $\pm$  S.E.) in  $E^+O^+$  individuals and  $6.8 \pm 1.2$  in  $E^+O^-$  treated individuals (Table 1). The spatial resolving power in  $E^+O^+$  individuals was  $0.29 \pm 0.02$  cpd (mean  $\pm$  SE) and  $0.21 \pm 0.01$ cpd in  $E^+O^-$  treated individuals (Table 1). The contrast sensitivity functions, the maximum contrast sensitivities, and the spatial resolving powers were significantly higher in  $E^+O^+$  individuals compared to  $E^+O^-$  treated individuals (Tables 2, 3, 4).

### **Contrast sensitivity in visual systems-intact individuals of *Myrmecia* ants and *Apis mellifera***

We measured the contrast sensitivity of the ocellar second-order neurons in four *Myrmecia* species and in the European honeybee *Apis mellifera* in  $E^+O^+$  individuals (Fig. 4). The contrast sensitivity decreased as the spatial frequency increased in all species (Fig. 4A, Table 5). The maximum contrast sensitivities attained at the lowest spatial frequency (0.05cpd) was highest in *M. midas* at  $16 \pm 1.2$  (6.3%) (mean  $\pm$  S.E.) to the lowest in *A. mellifera* at  $9.2 \pm 1.3$  (10.8%) (Table 1). Among the ants, a linear model of the maximum contrast sensitivities as a function of species showed that the maximum contrast sensitivities did not differ significantly between the species ( $F_{3,14} = 0.84$ ,  $P = 0.49$ ). Additionally, the variation in contrast sensitivity function was explained by the spatial frequency of the gratings, but not by the species or their time of activity (Table 5).

Since *Apis mellifera* is a flying diurnal species, we compared its contrast sensitivity function with that of *M. gulosa* and *M. tarsata* which are also active under bright-light conditions but use walking as their primary mode of locomotion. We found that the variation in contrast sensitivity function was explained by the spatial frequency of the gratings, but not by the species or their mode of locomotion (Table 6).

## Spatial resolving power in visual systems-intact individuals of *Myrmecia* ants and *Apis mellifera*

The spatial resolving power of the ocellar second-order neurons in the five species was measured in  $E^+O^+$  individuals (Fig. 4B). Among the five species, *M. pyriformis* had the lowest spatial resolving power at  $0.25 \pm 0.05$  cpd (mean  $\pm$  S.E.) and *M. gulosa* had the highest at  $0.34 \pm 0.02$  cpd (Table 1), but this variation was not significantly different between species (Linear model:  $F_{4,19}=0.93$ ,  $P=0.47$ ).

## Discussion

### Electroretinogram

To confirm the presence of the extracellular potentials from the ocellar second-order neurons in our ERG recordings, we measured ERGs responding to the ON-OFF stimuli from the ocellar retina of *M. tarsata* for  $E^+O^+$  and  $E^-O^+$  treated individuals (Fig. 1A). Similar to the ocellar ERGs in other insects (Ruck, 1961a; Ruck, 1961b), we found the presence of a hyperpolarizing post-synaptic potential and a sustained after-potential identified as Component 3 at the stimulus onset (Fig. 1B) and offset (Fig. 1C) respectively for  $E^+O^+$  individuals. In  $E^-O^+$  treated individuals, the sustained after-potential identified as part of Component 3 was seen at the stimulus offset (Fig. 1C). This confirms the presence of ERGs from the ocellar second-order neurons in our pERG recordings. As mentioned earlier, some L-neurons are known to interact with descending interneurons which receive input from the compound eyes (e.g., Strausfeld, 1976). We suspect that the presence of these descending interneurons along with the ocellar second-order neurons may explain the presence of Component 3 at both offset and onset in  $E^+O^+$  individuals. However, when the compound eyes are occluded ( $E^-O^+$ ), the ocellar second-order neurons alone produce Component 3 at the stimulus offset, although the Component 3 was absent at the stimulus onset.

### Contribution of the two visual systems to the pERG response amplitude

In order to evaluate the contribution of the signals from the compound eyes and the ocelli to the ocellar second-order neurons, we measured the pERG response amplitudes in  $E^+O^+$ ,  $E^+O^-$ ,  $E^-O^+$  and  $E^+O^+L^-$  treated individuals of *M. tarsata* (Fig. 2). The mean response amplitudes at the lowest spatial frequency (0.05 cpd) were higher in conditions when the compound eyes were intact (Fig. 2A, 2C) compared to conditions when the compound eyes were occluded or their neural input disrupted (Fig. 2B, 2D). This indicates that the compound

eyes contribute highly to the response amplitude of the ocellar second-order neurons. Furthermore, although the response amplitudes overall were not significantly different between  $E^+O^-$  and  $E^+O^+$  individuals, we found that at the lowest spatial frequency (0.05cpd) the mean response amplitudes was higher in  $E^+O^-$  treated individuals (Fig. 2C) than in  $E^+O^+$  individuals (Fig. 2A) with the difference close to being statistically significant. This raises the possibility that lower spatial frequencies might trigger an inhibitory response by the ocellar photoreceptors onto the ocellar second-order neurons. As seen in locusts, light intensity-dependent control of phototactic tuning tendencies occurs due to photoinhibition through the ocelli and photoexcitation through the compound eyes (Barry and Jander, 1968). This has been suggested to be a form of central light intensity adaptation (Barry and Jander, 1968). However, further physiological, neuroanatomical and behavioural evidence is required to confirm any inhibitory mechanisms by the ocelli in the context of spatial vision and its possible ecological relevancy.

The compound eyes' contribution to ocellar second-order neurons in ants may be explained by the neural pathways discussed previously. In various insect species, certain L-neurons are known to interact with descending interneurons (e.g., Strausfeld, 1976). We suspect a similar pathway is present in the ants studied. Additionally, the scale of the contribution of the compound eyes (Fig. 2A, C) was unexpectedly higher compared to the contribution of the ocelli to the ocellar second-order neurons (Fig. 2B). This may simply be a consequence of the high light capturing ability of the compound eyes owing to its multi-lens structure with a large number of facets (*M. tarsata*:  $2724 \pm 67$  facets/eye) (Greiner et al., 2007) and therefore numerous rhabdoms. This is drastically different when compared to the ocelli that consists of a single but large lens and has fewer rhabdoms (*M. tarsata*:  $46.5 \pm 7$  rhabdoms in the median ocelli) (Narendra and Ribi, 2017). Overall, insects with both visual systems appear to largely use their compound eyes to obtain sufficient spatial resolution and sensitivity in order to perform various visually guided behaviours.

Incidentally, the mean response amplitude at the lowest spatial frequency (0.05cpd) was significantly higher in  $E^-O^+$  individuals (Fig. 2B) than in  $E^+O^+L^-$  individuals (Fig. 2D). These differences may be due to the disruption in the neural pathway in  $E^+O^+L^-$  treated individuals. Consequently, this method was more effective to block the compound eyes' input than the compound eyes' occlusion done using black paint in the  $E^-O^+$  individuals.

Although the sample size for some of our treatment conditions were low, the standard errors of our data set were also low, indicating low data spread, further suggesting that physiological processes are conserved across individuals.

### Ocellar contrast sensitivity in *M. tarsata*

Due to the extremely low pERG response amplitudes from the ocellar second-order neurons of the  $E^-O^+$  treated individuals (Fig. 2B), it was not possible to directly measure the contribution of the ocelli to the contrast sensitivity and the spatial resolving power of the ocellar second-order neurons in *M. tarsata*. However, the high pERG response amplitudes in the  $E^+O^+$  treated individuals (Fig. 2A) and  $E^+O^-$  treated individuals (Fig. 2C) enabled us to estimate the visual capabilities of the ocelli. We found that the contrast sensitivity function and the maximum contrast sensitivity of ocellar second-order neurons were significantly different in  $E^+O^+$  and  $E^+O^-$  treated individuals. The mean maximum contrast sensitivity was higher in  $E^+O^+$  treated individuals ( $13 \pm 1.2$  (7.7%), mean  $\pm$  SE) than that in  $E^+O^-$  treated individuals ( $6.8 \pm 1.2$  (14.8%)), indicating a significant contribution of the ocelli to contrast sensitivity of the ocellar second-order neurons. This demonstrates that inputs from both the ocelli and the compound eyes contribute to the contrast sensitivity of the ocellar second-order neurons.

We speculate that in ants the descending interneurons receive information from the ocelli first and subsequently from the compound eyes. This is quite possible due to the fast transmission of signals via the L-neurons found in several insects (Guy et al., 1979; Mizunami, 1995). This could either modulate or gate the signals from the compound eyes (Guy et al., 1979). The input from the compound eyes could further increase the contrast sensitivity of the ocelli to enable efficient navigation (e.g., Fent and Wehner, 1985b; Schwarz et al., 2011b). Increased contrast sensitivity of the ocellar second-order neurons based on the contribution of the compound eyes together with the fast transmission of signals through the L-neurons would be beneficial for navigation and other visually guided behaviours (e.g., Barry and Jander, 1968; Cornwell, 1955; Honkanen et al., 2018; Lindauer and Schricker, 1963; Schricker, 1965; Wellington, 1974)

### Ocellar spatial resolving power in *M. tarsata*

The spatial resolving power of the ocellar second-order neurons in  $E^+O^+$  individuals ( $0.29 \pm 0.02$  cpd) and  $E^+O^-$  treated individuals ( $0.21 \pm 0.01$  cpd, Fig. 3B) were significantly different. Although a large number of ocellar photoreceptors converge onto very few ocellar second-order neurons (Berry et al., 2006; Chappell et al., 1978; Goodman and Williams, 1976; Guy et al., 1979; Mizunami, 1995; Patterson and Chappell, 1980; Toh and Kuwabara, 1974), in dragonflies the spatial resolution is conserved even after this convergence indicating the possibility of local processing within the ocellar neuropil (Berry et al., 2006).

Our results suggest that in ants, the ocellar second-order neurons are involved in processing such that they contribute to ocellar spatial vision to some extent but its functional significance remains to be investigated. It is likely that the ocellar spatial acuity is enhanced when there is input from the both the ocelli and compound eyes.

### **Spatial properties of the ocellar second-order neurons in ants and honeybees**

Nocturnal *Myrmecia* ants have larger ocelli and wider ocellar rhabdoms (Narendra and Ribi, 2017) compared to their diurnal relatives, indicating that the ocelli might have higher contrast sensitivities. Therefore, we compared the contrast sensitivities of the ocellar second-order neurons in  $E^+O^+$  individuals of *Myrmecia* species active at discrete times of the day (Fig. 4). However, the contrast sensitivity functions were not significantly different between the species, indicating that the time of activity did not have an effect on their contrast sensitivity functions. This is consistent with our knowledge of the compound eyes, where the time of activity does not explain the difference in contrast sensitivities of the compound eyes of diurnal and nocturnal *Myrmecia* ants (Ogawa et al., 2019).

To identify whether ocellar spatial properties were affected by the mode of locomotion, we studied the diurnal flying European honeybee *A. mellifera* ( $E^+O^+$ ) and compared it with diurnal *Myrmecia* ants. We chose *A. mellifera* because their ocelli have been well studied: interaction with the compound eyes has been mapped (Guy et al., 1979); the plane of best focus is known to lie on the ocellar retina (Ribi et al., 2011). With ocellar lens diameters of 294  $\mu\text{m}$ , *A. mellifera* (Ribi et al., 2011) have distinctly larger ocelli than the *Myrmecia* ants (*M. tarsata*: 129.2  $\mu\text{m}$  (Narendra and Ribi, 2017)). Our results showed that the species and their locomotion did not have an effect on their contrast sensitivity functions.

Based on our experimental paradigm, we suspect that the main function of the ocellar second-order neurons for  $E^+O^+$  individuals in all five species is to detect overall bright and dim contrasts, indicating that the overall processing of visual information is similar in their peripheral neural pathways. However, it must be stated that the contrast sensitivities of species may change depending on the intensity of light present. Our results are reflective of contrast sensitivities at a particular light intensity and may differ at different light intensities. In future, different species can be compared by measuring the response-stimulus intensity ( $V\text{-log } I$ ) functions. The saturation and adaptation levels of the photoreceptors can also be assessed using this method.

The spatial resolving powers of the ocellar second-order neurons of *Myrmecia* ants and that of *Apis mellifera* for E<sup>+</sup>O<sup>+</sup> individuals measured in this study were not significantly different between species. The neural pathways relaying information from the compound eyes to the ocellar second-order neurons are likely to be conserved across all the five Hymenopteran species leading to the lack of difference in spatial resolving power in all species.

In conclusion, our results provide physiological evidence that the compound eyes modulate the signals generated by the ocelli and, therefore, significantly affect the contrast sensitivity of the median ocelli and subsequently the spatial resolving power, with a noticeably larger improvement in contrast sensitivity than in spatial resolving power. The functional significance of this modulation, and how it affects visually guided behaviours, remains to be discovered.

### **Diversity and Inclusion Statement**

We strongly support equity, diversity and inclusion in science. The authors come from different countries (India, Japan, Australia, and the United Kingdom) and represent different career stages (PhD Candidate, Postdoctoral Researcher, Senior Lecturer, Professor). Three of the authors are from underrepresented ethnic minorities in science. Three of the authors self-identify as female, an underrepresented gender in science. While citing references scientifically relevant for this work, we actively worked to promote gender balance in our reference list as much as possible.

### **Acknowledgements**

We thank Ken Cheng and Chris Reid for their comments on an earlier version of the manuscript. We acknowledge the *Wallumattagal clan of the Dharug nation* as the traditional custodians of the Macquarie University land. We conducted research on the lands of the *Dharug* people and collected specimen from the lands of the *Dharug* and *Darkinjung* people.

### **Competing interests**

The authors declare no competing or financial interests.

## Author contributions

Study design: B.P., Y.O., A.N.; Data collection and analyses: B.P., Y.O., L.R.; Built the equipment and wrote the software: N.H., L.R., Y.O.; Writing – original draft: B.P.; Writing – review and editing: all authors; Visualisation: B.P., Y.O., A.N.; Funding acquisition: A.N.

## Funding

We acknowledge financial support from the Australian Research Council, Discovery Project grants (DP150101172, DP200102337) and Future Fellowship (FT140100221) and Hermon Slade Foundation (HSF17/08). B.P. was supported by the International Macquarie Research Excellence Scholarship.

## Data Availability

Raw data used for this study can be accessed at:

[https://ecologicalneuroscience.files.wordpress.com/2021/08/penmetcha\\_etal\\_2021\\_dataset.xlsx](https://ecologicalneuroscience.files.wordpress.com/2021/08/penmetcha_etal_2021_dataset.xlsx)

## References

- Bates D, Mächler M, Bolker B, Walker S (2015).** Fitting Linear Mixed-Effects Models using lme4. *J. Stat. Softw.* **67**, 1–48.
- Barry, C. K. and Jander, R. (1968).** Photoinhibitory function of the dorsal ocelli in the phototactic reaction of the migratory locust *Locusta migratoria* L. *Nature* **217**, 675–677.
- Berry, R., Stange, G., Olberg, R. and Van Kleef, J. (2006).** The mapping of visual space by identified large second-order neurons in the dragonfly median ocellus. *J. Comp. Physiol. A* **192**, 1105–1123.
- Berry, R., Van Kleef, J. and Stange, G. (2007a).** The mapping of visual space by dragonfly lateral ocelli. *J. Comp. Physiol. A* **193**, 495–513.
- Berry, R. P., Warrant, E. J. and Stange, G. (2007b).** Form vision in the insect dorsal ocelli: An anatomical and optical analysis of the locust ocelli. *Vision Res.* **47**, 1382–1393.

- Berry, R. P., Stange, G. and Warrant, E. J.** (2007c). Form vision in the insect dorsal ocelli: An anatomical and optical analysis of the dragonfly median ocellus. *Vision Res.* **47**, 1394–1409.
- Chappell, R. L., Goodman, L. J. and Kirkham, J. B.** (1978). Lateral ocellar nerve projections in the dragonfly brain. *Cell Tissue Res.* **190**, 99–114.
- Coombe, P. E.** (1986). The large monopolar cells L1 and L2 are responsible for ERG transients in *Drosophila*. *J. Comp. Physiol. A* **159**, 655–665.
- Cornwell, P. B.** (1955). The functions of the ocelli of *Calliphora* (Diptera) and *Locusta* (Orthoptera). *J. Exp. Biol.* **32**, 217–237.
- Cronin, T. W., Johnsen, S., Marshall, N. J. and Warrant, E. J.** (2014). *Visual Ecology*. Princeton, New Jersey: Princeton University Press.
- Fent, K. and Wehner, R.** (1985). Ocelli: A celestial compass in the desert ant *Cataglyphis*. *Science*. **228**, 192–194.
- Freas, C. A., Narendra, A. and Cheng, K.** (2017). Compass cues used by a nocturnal bull ant, *Myrmecia midas*. *J. Exp. Biol.* **220**, 1578–1585.
- Goodman, C. and Williams, J.** (1976). Anatomy of the ocellar interneurons of acridid grasshoppers. *Cell Tissue Res.* **225**, 203–225.
- Greiner, B.** (2006). Adaptations for nocturnal vision in insect apposition eyes. *Int. Rev. Cytol.* **250**, 1–46.
- Greiner, B., Narendra, A., Reid, S. F., Dacke, M., Ribi, W. A. and Zeil, J.** (2007). Eye structure correlates with distinct foraging-bout timing in primitive ants. *Curr. Biol.* **17**, 879–880.
- Guy, R. G., Goodman, L. J. and Mobbs, P. G.** (1979). Visual interneurons in the bee brain: synaptic organisation and transmission by graded potentials. *J. Comp. Physiol. A* **134**, 253–264.
- Hagberg, M. and Nässel, D. R.** (1986). Interneurones subserving ocelli in two species of trichopterous insects: morphology and central projections. *Cell Tissue Res.* **245**, 197–205.
- Homann, H.** (1924). Zum problem der ocellenfunktion bei den insekten. *Z. Vgl. Physiol.* **1**, 541–578.
- Honegger, H. W. and Schürmann, F. W.** (1975). Cobalt sulphide staining of optic fibres in the brain of the cricket, *Gryllus campestris*. *Cell Tissue Res.* **159**, 213–225.
- Honkanen, A., Saari, P., Takalo, J., Heimonen, K. and Weckström, M.** (2018). The role of ocelli in cockroach optomotor performance. *J. Comp. Physiol. A* **204**, 231–243.

- Hung, Y.-S. and Ibbotson, M. R.** (2014). Ocellar structure and neural innervation in the honeybee. *Front. Neuroanat.* **8**, 1–11.
- Land, M. F.** (1989). Variations in the structure and design of compound eyes. In *Facets of Vision* (ed. Stavenga, D. G. and Hardie, R. C.), pp. 90–111. Berlin, Germany: Springer.
- Land, M. F.** (1997). Visual acuity in insects. *Annu. Rev. Entomol.* **42**, 147–77.
- Mizunami, M.** (1995). Information processing in the insect ocellar system: comparative approaches to the evolution of visual processing and neural circuits. *Adv. In Insect Phys.* **25**, 151–152.
- Mote, M. I. and Wehner, R.** (1980). Functional characteristics of photoreceptors in the compound eyes and ocellus of the desert ant, *Cataglyphis bicolor*. *J. Comp. Physiol. A* **137**, 63–71.
- Narendra, A. and Ribi, W. A.** (2017). Ocellar structure is driven by the mode of locomotion and activity time in *Myrmecia* ants. *J. Exp. Biol.* **220**, 4383–4390.
- Narendra, A., Reid, S. F. and Hemmi, J. M.** (2010). The twilight zone: ambient light levels trigger activity in primitive ants. *Proc. R. Soc. B* **277**, 1531–1538.
- Narendra, A., Reid, S. F., Greiner, B., Peters, R. A., Hemmi, J. M., Ribi, W. A. and Zeil, J.** (2011). Caste-specific visual adaptations to distinct daily activity schedules in Australian *Myrmecia* ants. *Proc. R. Soc. B* **278**, 1141–1149.
- Narendra, A., Kamhi, J. F. and Ogawa, Y.** (2017). Moving in dim light: behavioral and visual adaptations in nocturnal ants. *Integr. Comp. Biol.* **57**, 1104–1116.
- Ogawa, Y., Ryan, L. A., Palavalli-Nettimi, R., Seeger, O., Hart, N. S. and Narendra, A.** (2019). Spatial resolving power and contrast sensitivity are adapted for ambient light conditions in Australian *Myrmecia* ants. *Front. Ecol. Evol.* **7**, 1–10.
- Palavalli-Nettimi, R., Ogawa, Y., Ryan, L. A., Hart, N. S. and Narendra, A.** (2019). Miniaturisation reduces contrast sensitivity and spatial resolving power in ants. *J. Exp. Biol.* **222**, 1–10.
- Patterson, J. A. and Chappell, R. L.** (1980). Intracellular responses of procion filled cells and whole nerve cobalt impregnation in the dragonfly median ocellus. *J. Comp. Physiol. A* **139**, 25–39.
- Pelli G Denis** (1997). The VideoToolbox software for visual psychophysics: transforming numbers in movies. *Spat. Vis.* **10**, 437–442.
- Penmetcha, B., Ogawa, Y., Ribi, W. A. and Narendra, A.** (2019). Ocellar structure of African and Australian desert ants. *J. Comp. Physiol. A* **205**, 699–706.
- Porciatti, V.** (2007). The mouse pattern electroretinogram. *Doc. Ophthalmol.* **115**, 145–153.

- R Core Team** (2018). R: A language and environment for statistical computing.
- Rence, B. G., Lisý, M. T., Garves, B. R. and Quinlan, B. J.** (1988). The role of ocelli in circadian singing rhythms of crickets. *Physiol. Entomol.* **13**, 201–212.
- Ribi, W. A. and Zeil, J.** (2018). Diversity and common themes in the organization of ocelli in Hymenoptera, Odonata and Diptera. *J. Comp. Physiol. A* **204**, 505–517.
- Ribi, W. A., Warrant, E. J. and Zeil, J.** (2011). The organization of honeybee ocelli: regional specializations and rhabdom arrangements. *Arthropod Struct. Dev.* **40**, 509–520.
- Rowell, C. and Pearson, K.** (1983). Ocellar input to the flight motor system of the locust: structure and function. *J. Exp. Biol.* **103**, 265–288.
- Ruck, P.** (1961a). Electrophysiology of the insect dorsal ocellus. I. Origin of the components of the electroretinogram. *J. Gen. Physiol.* **44**, 605–627.
- Ruck, P.** (1961b). Electrophysiology of the insect dorsal ocellus. II. Mechanisms of generation and inhibition of impulses in the ocellar nerve of dragonflies. *J. Gen. Physiol.* **44**, 629–639.
- Ryan, L. A., Cunningham, R., Hart, N. S. and Ogawa, Y.** (2020). The buzz around spatial resolving power and contrast sensitivity in the honeybee, *Apis mellifera*. *Vision Res.* **169**, 25–32.
- Schricker, B.** (1965). Die orientierung der honigbiene in der dämmerung. *Z. Vgl. Physiol.* **49**, 420–458.
- Schuppe, H. and Hengstenberg, R.** (1993). Optical properties of the ocelli of *Calliphora erythrocephala* and their role in the dorsal light response. *J. Comp. Physiol. A* **173**, 143–149.
- Schwarz, S., Narendra, A. and Zeil, J.** (2011a). The properties of the visual system in the Australian desert ant *Melophorus bagoti*. *Arthropod Struct. Dev.* **40**, 128–134.
- Schwarz, S., Wystrach, A. and Cheng, K.** (2011b). A new navigational mechanism mediated by ant ocelli. *Biol. Lett.* **7**, 856–858.
- Schwarz, S., Albert, L., Wystrach, A. and Cheng, K.** (2011c). Ocelli contribute to the encoding of celestial compass information in the Australian desert ant *Melophorus bagoti*. *J. Exp. Biol.* **214**, 901–906.
- Sheehan, Z. B. V., Kamhi, J. F., Seid, M. A. and Narendra, A.** (2019). Differential investment in brain regions for a diurnal and nocturnal lifestyle in Australian *Myrmecia* ants. *J. Comp. Neurol.* **527**, 1–17.

- Simmons, P. J.** (1993). Adaptation and responses to changes in illumination by second- and third-order neurones of locust ocelli. *J. Comp. Physiol. A* **173**, 635–648.
- Somanathan, H., Kelber, A., Borges, R. M., Wallén, R. and Warrant, E. J.** (2009). Visual ecology of Indian carpenter bees II: adaptations of eyes and ocelli to nocturnal and diurnal lifestyles. *J. Comp. Physiol. A* **195**, 571–583.
- Stange, G.** (1981). The ocellar component of flight equilibrium control in dragonflies. *J. Comp. Physiol. A* **141**, 335–347.
- Stange, G., Stowe, S., Chahl, J. S. and Massaro, A.** (2002). Anisotropic imaging in the dragonfly median ocellus: a matched filter for horizon detection. *J. Comp. Physiol. A* **188**, 455–467.
- Strausfeld, N. J.** (1976). *Atlas of an Insect Brain*. Berlin, Heidelberg: Springer.
- Strausfeld, N. J. and Bassemir, U. K.** (1985). Lobula plate and ocellar interneurons converge onto a cluster of descending neurons leading to neck and leg motor neuropil in *Calliphora erythrocephala*. *Cell Tissue Res.* **240**, 617–640.
- Taylor, C. P.** (1981). Contribution of compound eyes and ocelli to steering of locusts in flight: I. Behavioural analysis. *J. Exp. Biol.* **93**, 1–18.
- Taylor, G. J., Ribi, W. A., Bech, M., Bodey, A. J., Rau, C., Steuwer, A., Warrant, E. J. and Baird, E.** (2016). The dual function of Orchid bee ocelli as revealed by X-ray microtomography. *Curr. Biol.* **26**, 1319–1324.
- Toh, Y. and Kuwabara, M.** (1974). Fine structure of the dorsal ocellus of the worker honeybee. *J. Morphol.* **143**, 285–305.
- van Kleef, J., James, A. C. and Stange, G.** (2005). A spatiotemporal white noise analysis of photoreceptor responses to UV and green light in the dragonfly median ocellus. *J. Gen. Physiol.* **126**, 481–497.
- Warrant, E. J.** (2008). Seeing in the dark: vision and visual behaviour in nocturnal bees and wasps. *J. Exp. Biol.* **211**, 1737–1746.
- Warrant, E. J., Kelber, A., Wallén, R. and Wcislo, W. T.** (2006). Ocellar optics in nocturnal and diurnal bees and wasps. *Arthropod Struct. Dev.* **35**, 293–305.
- Wellington, W.** (1974). Bumblebee ocelli and navigation at dusk. *Science*. **183**, 551–552.
- Wilson, M.** (1978). The functional organisation of locust ocelli. *J. Comp. Physiol. A* **124**, 297–316.

## Figures

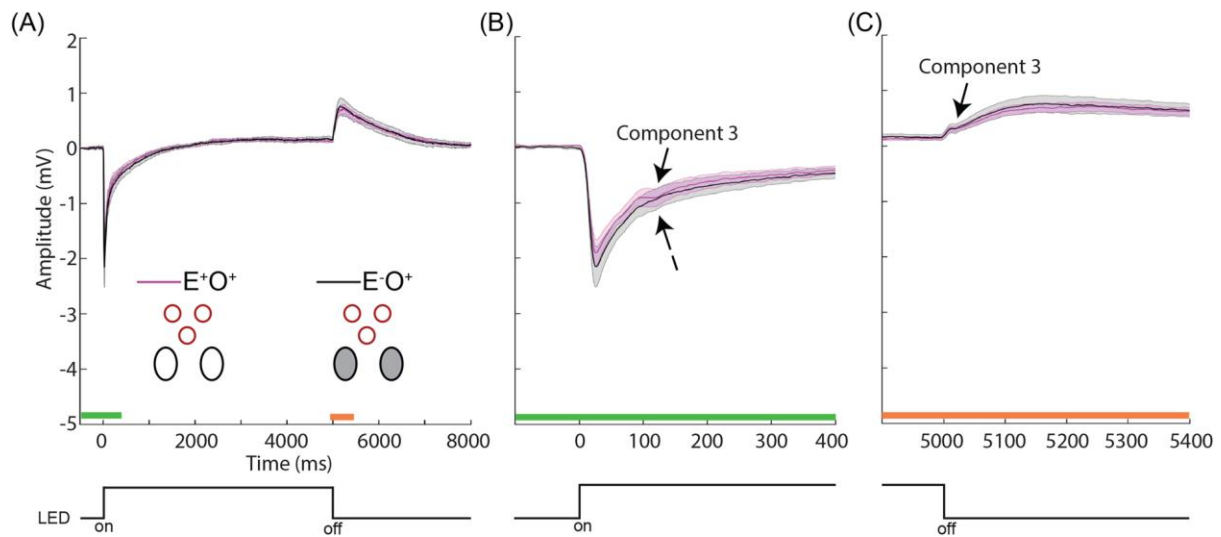


**Figure 1. Electrophysiological recordings from median ocelli of *Myrmecia tarsata* for visual systems-intact ( $E^+O^+$ ) and compound eyes-occluded ( $E^-O^+$ ) individuals.** Mean ERGs from ocelli in response to ON-OFF LED light stimulus for visual systems-intact ( $E^+O^+$ ,  $n=5$ ) individuals are shown in pink and for that of compound eyes-occluded ( $E^-O^+$ ,  $n=5$ ) individuals are shown in black. The shaded regions show the standard error for the respective conditions. Solid arrows indicate presence of Component 3. Dashed arrow shows that Component 3 is absent in  $E^-O^+$  treated individuals. Stimulus onset and offset represented at the bottom. **(A)** ERGs for  $E^+O^+$  and  $E^-O^+$  treated individuals. Green bar indicates time scale magnified and presented in **(B)** and orange bar indicates time scale magnified and presented in **(C)**. Pictograms represent treatment condition: ovals: compound eyes; circles: ocelli. Filled symbols: occlusion; open symbols: no occlusion.

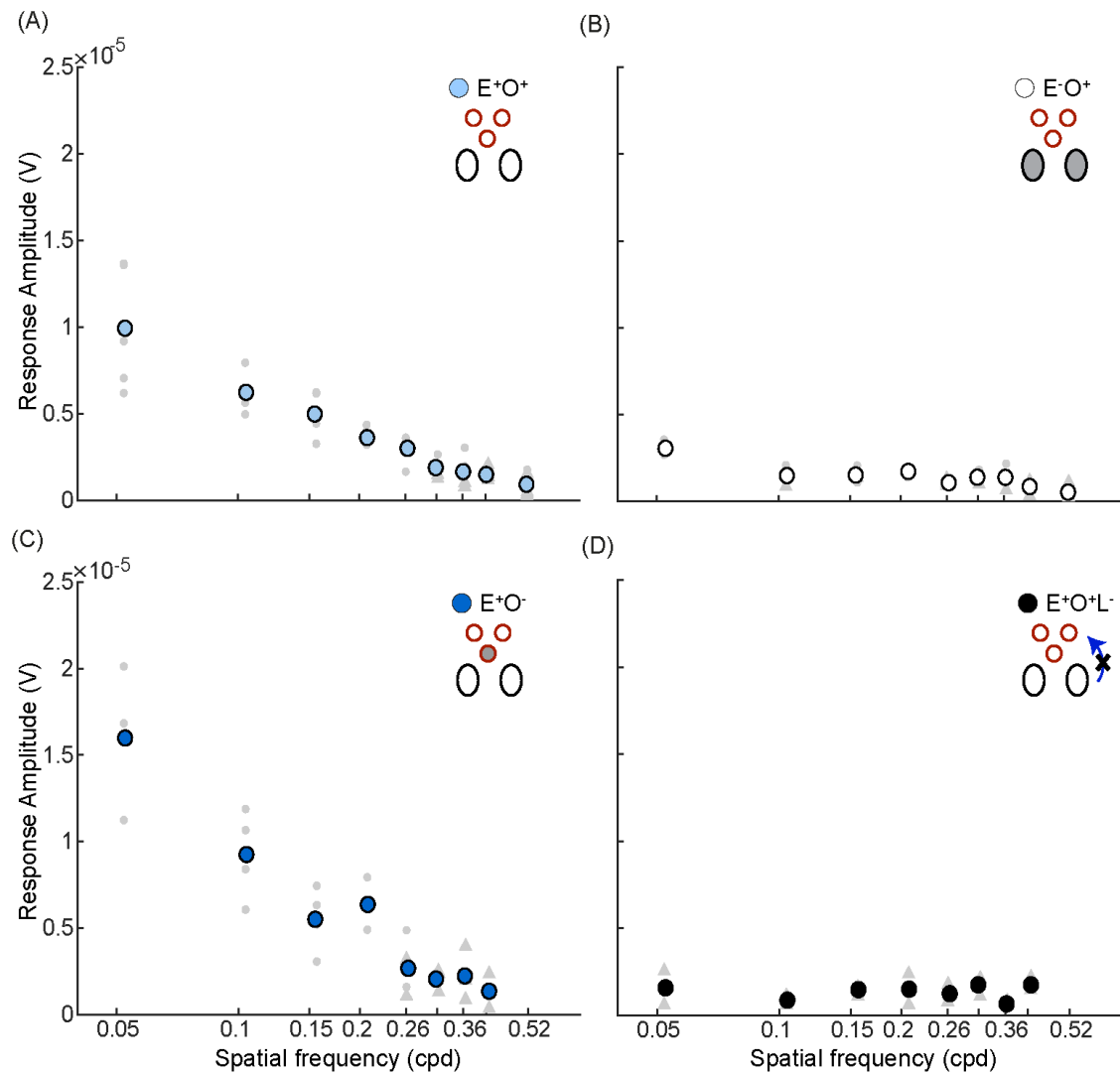


**Figure 2. Amplitude of pERG response signal from the ocellar second-order neurons of *Myrmecia tarsata* under different treatment conditions.** (A) Visual systems-intact individuals ( $E^+O^+$ ), (B) Compound eyes-occluded individuals ( $E^-O^+$ ), (C) Ocelli-occluded individuals ( $E^+O^-$ ), (D) Visual systems-intact individuals with incisions made in the lamina ( $E^+O^+L^-$ ) (see methods for details). Each coloured data point is the mean amplitude of the signal of all individuals at the corresponding spatial frequency at 95% contrast. Individual significant data points (see methods) shown in grey circles. Individual non-significant data points (see methods) shown in grey triangles. ( $n=5$  for  $E^+O^+$ ,  $n=4$  for  $E^-O^+$ ,  $n=3$  for  $E^+O^-$ ,  $E^+O^+L^-$ ). Pictograms represent treatment condition: ovals: compound eyes; circles: ocelli. Filled symbols: occlusion; open symbols: no occlusion. Note, only the median ocellus was stimulated in all experiments.

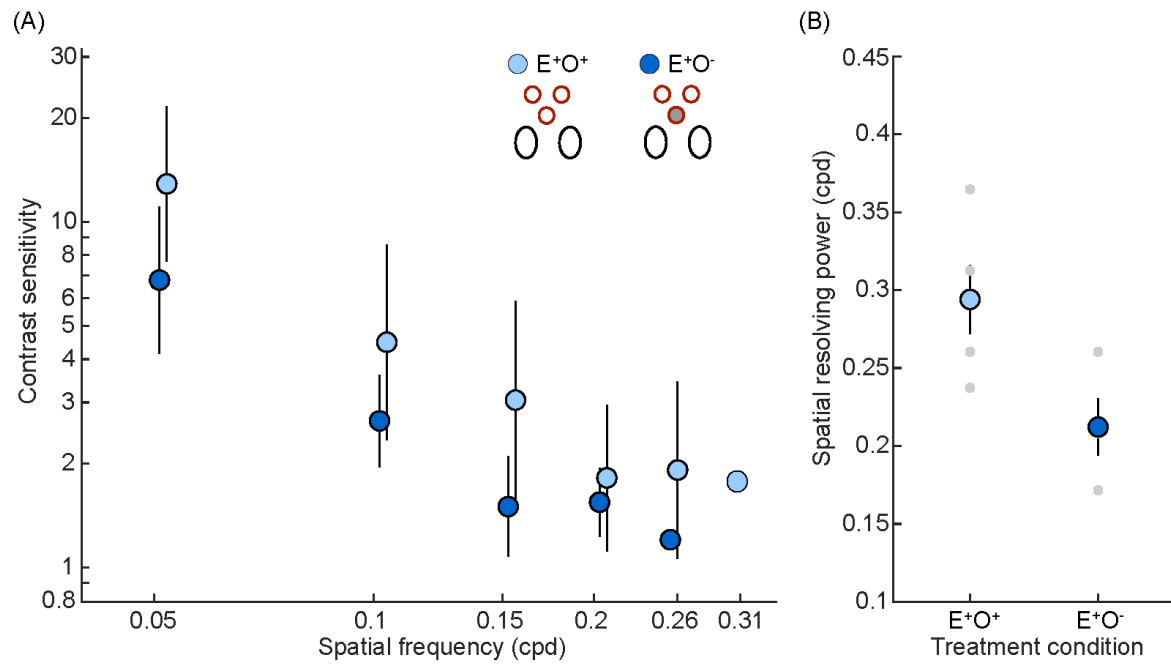


**Figure 3. Spatial properties of ocellar second-order neurons of *Myrmecia tarsata* for visual systems-intact individuals ( $E^+O^+$ ) and, ocelli-occluded individuals ( $E^+O^-$ ). (A) Contrast sensitivity function and (B) Spatial resolving power for the two treatment conditions are shown. In Panel A, each data point is the mean contrast sensitivity of all individuals of *M. tarsata* for a particular treatment condition at the corresponding spatial frequency. The error bars show 95% confidence intervals. Data points for each condition were shifted to the right or left of the recorded spatial frequency to improve visualisation. (B) Each coloured data point is the mean spatial resolving power of all individuals of *M. tarsata* for a particular condition at 95% contrast. Error bars show standard error. Individual data points are shown in grey. Pictogram descriptions as mentioned in Figure 2 (n=5 for  $E^+O^+$ , n=4 for  $E^+O^-$ ).**

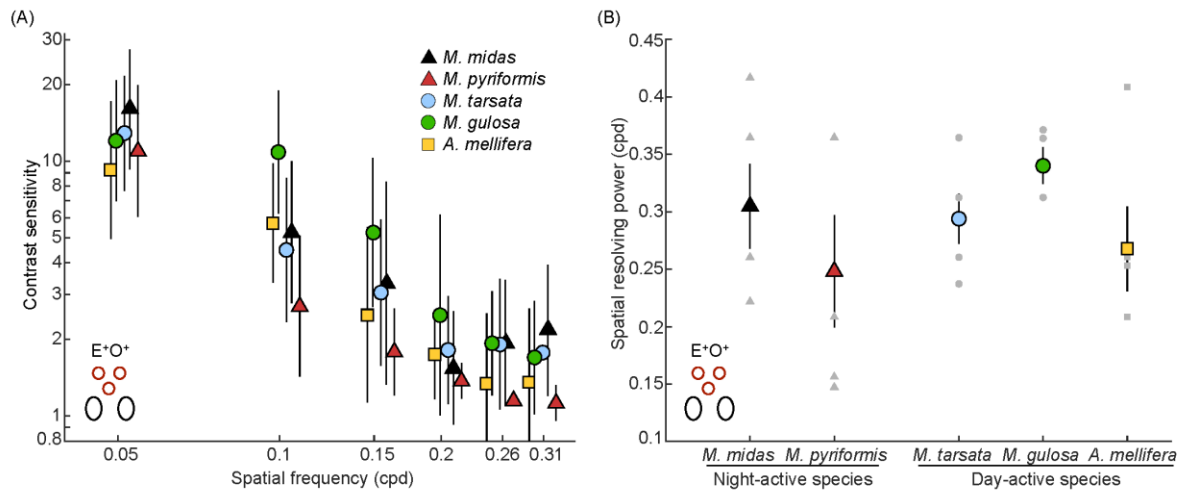


**Figure 4. Spatial properties of ocellar second-order neurons of four *Myrmecia* species and *Apis mellifera* for visual systems-intact individuals ( $E^+O^+$ ) (A) Contrast sensitivity and (B) Spatial resolving power for each species are shown. In Panel A, each data point is the mean contrast sensitivity of all individuals of a particular species at the corresponding spatial frequency. The error bars show 95% confidence intervals. Data points for each species were shifted to the right or left of the recorded spatial frequency to improve visualisation. (B) Each coloured data point is the mean spatial resolving power of all individuals of a particular species at 95% contrast. Error bars show standard error. Individual data points are shown in grey. Triangles indicate nocturnal ant species, circles indicate diurnal-crepuscular ant species. Pictogram descriptions as mentioned in Figure 2. (n=4 for *M. gulosa*, n=5 for remaining species).**

**Table 1. Summary of spatial resolving power and contrast sensitivity of ocellar second-order neurons for *Apis mellifera* and *Myrmecia* ants under different treatment conditions**

	<i>M. tarsata</i>	<i>M. tarsata</i>	<i>M. gulosa</i>	<i>M. midas</i>	<i>M. pyriformis</i>	<i>A. mellifera</i>
	diurnal- crepuscular	diurnal- crepuscular	diurnal- crepuscular	nocturnal	nocturnal	diurnal
	walking	walking	walking	walking	walking	flying
	(n=4)	(n=5)	(n=4)	(n=5)	(n=5)	(n=5)
Treatment condition	E <sup>+</sup> O <sup>-</sup>	E <sup>+</sup> O <sup>+</sup>				
Spatial resolving power (cpd), (mean ± S.E.)	0.21 ± 0.01	0.29 ± 0.02	0.34 ± 0.02	0.30 ± 0.04	0.25 ± 0.05	0.27 ± 0.04
Maximum contrast sensitivity (mean ± S.E.)	6.8 ± 1.2 (14.8%)	13 ± 1.2 (7.7%)	12 ± 1.2 (8.3 %)	16 ± 1.2 (6.3%)	11 ± 1.2 (9.1%)	9.2 ± 1.3 (10.8%)

E<sup>+</sup>O<sup>-</sup> = ocelli-occluded individuals; E<sup>+</sup>O<sup>+</sup> = visual systems-intact individuals

**Table 2. Summary of linear mixed-effects model analysis for testing the effect of spatial frequency of gratings and treatment condition ( $E^+O^+$  and  $E^+O^-$ ) on contrast sensitivity functions in *M. tarsata*.** Model: contrast sensitivity  $\sim$  spatial frequency + treatment condition (1|animal ID). The *t*-tests for fixed effects use Satterthwaite approximations to degrees of freedom (*df*). The variance of each of the random effects is <3%

Parameter	Estimate	Standard Error	<i>Df</i>	<i>t</i> -value	<i>p</i> -value
Intercept	-0.5	0.09	35.74	-5.3	<6.03e-06
Spatial frequencies	-1.21	0.09	31.92	-12.98	<2.83e-14
Treatment condition	-0.24	0.07	7.22	-3.23	<0.01

**Table 3. Summary of the linear model for testing the relationship between maximum contrast sensitivity and treatment condition ( $E^+O^+$  and  $E^+O^-$ ) in *M. tarsata*.** Model: maximum contrast sensitivity  $\sim$  treatment condition

Parameter	Estimate	Standard Error	<i>t</i> -value	<i>p</i> -value
Intercept	0.1	0.07	15.25	0.000001
Treatment condition	-0.28	0.1	-2.55	<0.04

*Maximum contrast sensitivity* = - 0.28\**treatment condition* + 0.1

**Table 4. Summary of the linear model for testing the relationship between spatial resolving power and treatment condition ( $E^+O^+$  and  $E^+O^-$ ) in *M. tarsata*.** Model: spatial resolving power  $\sim$  treatment condition

Parameter	Estimate	Standard Error	<i>t</i> -value	<i>p</i> -value
Intercept	0.29	0.02	14.87	<1.49e-06
Treatment condition	-0.08	0.03	-2.75	<0.03

*Spatial resolving power* = - 0.08\**treatment condition* + 0.29

**Table 5. Summary of the linear mixed-effects model for testing the relationship between contrast sensitivity function of the ocellar second-order neurons, spatial frequency of gratings and time of activity in *Myrmecia* ants.** Model: contrast sensitivity ~ spatial frequency + time of activity + (1|species/animal ID). The *t*-tests for fixed effects use Satterthwaite approximations to degrees of freedom (*df*). The variance of each of the random effects is < 3%

Parameter	Estimate	Standard Error	<i>df</i>	<i>t</i> -value	<i>p</i> -value
Intercept	-0.57	0.09	3.47	-6.27	0.00524
Spatial frequency	-1.24	0.06	95.77	-22.04	<2e-16
Time of activity	0.12	0.11	2.01	1.05	0.4

**Table 6. Summary of the linear mixed-effects model for testing the relationship between contrast sensitivity function of the ocellar second-order neurons, spatial frequency of gratings and locomotion in diurnal *Myrmecia* ants and *Apis mellifera*.** Model: contrast sensitivity ~ spatial frequency + locomotion + (1|species/animal ID). The *t*-tests for fixed effects use Satterthwaite approximations to degrees of freedom (*df*). The variance of each of the random effects is < 3%

Parameter	Estimate	Standard Error	<i>df</i>	<i>t</i> -value	<i>p</i> -value
Intercept	-0.39	0.08	2.92	-4.8	0.02
Spatial frequency	-1.17	0.06	71.2	-17.74	<2e-16
Locomotion	-0.09	0.11	0.96	-0.86	0.55